Journal of Diabetes Research & Clinical Metabolism
ISSN 2050-0866 | Volume 4 | Article 4

HOAJ
Herbert Open Access Journals

Special Section | Endocrinology Mechanisms | Original Research Open Access

Further insight into the role of metals in amyloid formation by $IAPP_{1-37}$ and $ProIAPP_{1-48}$

Matthew Mold[1], Chayanit Bunrat[2], Priya Goswami[2], Adam Roberts[2], Charlotte Roberts[2], Navada Taylor[2], Hannah Taylor[2], Ling Wu[3], Paul E. Fraser[3] and Christopher Exley[1*]

*Correspondence: c.exley@keele.ac.uk

[1]The Birchall Centre, Lennard-Jones Laboratories, Keele University, Staffordshire, ST5 5BG, UK.
[2]The Huxley Building, Life Sciences, Keele University, Staffordshire, ST5 5BG, UK.
[3]Tanz Centre for Research in Neurodegenerative Diseases and Department of Medical Biophysics, University of Toronto, Toronto, Ontario, Canada.

Abstract

Background: $IAPP_{1-37}$ and $ProIAPP_{1-48}$ are amyloidogenic peptides implicated in β-cell death in diabetes. Interactions with metals may be involved in both the cytotoxicity of these peptides and their deposition as amyloids associated with diabetes-related pathologies.

Methods: We have used the complementary methods of thioflavin T (ThT) fluorescence and transmission electron microscopy (TEM) to investigate the role of seeds and specifically metal-peptide seeds in accelerating amyloid formation by ProIAPP. In addition we have used these complementary methods alongside dynamic light scattering (DLS) to observe the dynamics of IAPP amyloid formation during the earliest phase of peptide aggregation.

Results: Seeding universally resulted in an acceleration of amyloid formation, as indicated by increased ThT fluorescence, over the shorter term (minutes) while having no influence upon total amyloid deposits (no differences in ThT fluorescence) over many days. Only copper-peptide seeds were ineffective in accelerating amyloid formation above that observed for sham seeds (no peptide). Different seeding environments resulted in amyloid deposits of different fibrillar and non-fibrillar morphologies following longer term incubations regardless of the uniform nature of the respective measurements of ThT fluorescence. The aggregation dynamics of IAPP, mimicking its secretion into extracellular milieus, were complex and suggested that while metals at equimolar, generally increased rates of aggregation, with the possible exception of Cu(II), the range of sub-micron and micron-sized particles observed were not easily explained by either measurement of ThT fluorescence or imaging by TEM.

Conclusions: Seeding may be significant in accelerating the formation of amyloid and in influencing the final morphologies of deposited amyloids but not in determining the total deposits of amyloid. It was of interest that copper-peptide seeds did not accelerate amyloid formation in the shorter term and this could indicate an incompatible seeding morphology due to copper? This first attempt to monitor aggregation dynamics of IAPP over only minutes has shown direct impact of metals on peptide particle size which could have implications for the cytotoxicity of IAPP in diabetes.

Keywords: Diabetes, metals, amyloid, amylin, IAPP, ProIAPP, ThT fluorescence, TEM, DLS

Background

Amyloids derived from a burgeoning number of different peptides and proteins have been implicated in the aetiologies of human disease including neurodegenerative diseases, heart disease and diabetes [1]. In diabetes the peptides IAPP and ProIAPP are known to be amyloidogenic and are linked with cytotoxicity of β cells in the islets of Langerhans in the pancreas [2]. A universal mystery in amyloidogenesis is how amyloids form *in vivo* when the concentrations in extracellular milieus of their peptide or protein precursors are consistently

doi: 10.7243/2050-0866-4-4

below saturation. The role of metals in catalysing amyloidogenesis has been studied extensively and the propensities for both IAPP [3] and ProIAPP [4] to form amyloid β sheets are significantly influenced by metals. While the evidence is quite clear that Cu(II) prevents both IAPP and ProIAPP from forming amyloid β sheets the data pertaining to Al(III), Fe(III) and Zn(II) remains equivocal as to whether they promote or have little influence upon the formation of amyloid β sheets [3-8]. All metals do affect the morphologies of amyloid-like materials [4] and there are also suggestions that the subsequent aggregation of such materials towards precipitated solids is influenced by metals [9].

When IAPP and ProIAPP are released into extracellular milieus *in vivo* they are secreted as vesicle concentrates which will then dilute into the extracellular environment. Herein we have looked to mimic these conditions *in vitro* and to follow the subsequent dilution of peptide concentrates into extracellular fluids and thereafter their aggregation towards fibrillar and non-fibrillar deposits.

Methods

IAPP and ProIAPP$_{1-48}$ (no C-terminal fragment) were synthesised by standard FMOC-based solid phase methods using an Applied Biosystems 433A synthesiser and purified by RP HPLC using water/acetonitrile mixtures buffered with 0.1% TFA on a POROS 20R2 column. Peptide content was confirmed by quantitative amino acid analysis and lyophilised peptide stored at -80°C until required. Thawed peptides were dissolved in ultra-pure water (conductivity <0.067 μS/cm) to give peptide stocks of *ca* 200 μM. Peptide stocks were diluted into modified Krebs-Henseleit medium buffered at pH 7.40±0.05 [10] to give the required treatments and all assays and incubations were at 37°C. Metals were added from certified stock solutions (Perkin-Elmer, UK) prior to addition of peptide stocks. Similarly, citrate (1.0 mM) was added from a 10 mM stock of citric acid to KH media prior to both metals and peptides. Seeds of ProIAPP were prepared as equimolar solutions of peptide ± metal (75 μM) aged at 37°C for 24h prior to their addition to 100 μL assays as 5 μL aliquots. All peptide-containing seeds, with the exception of ProIAPP-Cu(II), showed significant ThT fluorescence (>100 AU) before their addition to assays. The presence of β sheets of amyloid in assays was followed by ThT fluorescence and TEM using established methods [10,11]. Peptide aggregation was followed at 37°C by dynamic light scattering (DLS) using the ZetaSizer NanoZS (Malvern Instruments, UK). The method relies upon Brownian motion to keep primarily sub-micron particles in suspension and measures peak intensities (%) for particles of diameter, nanometer (*ca* 1nm) to micrometer (<6 μm). Aliquots of peptide stocks were added to prepared KH media without any mixing or stirring prior to the capture of particle size data. Only assays which gave a count rate >75 counts per minute (cpm) and particles with intensity above 1% were included in the collected data.

Results

Influence of the metal:peptide ratio on ThT fluorescence of IAPP

All treatments were mixed by brief vortexing prior to sampling for ThT fluorescence. The co-incubation of 5 μM IAPP with Al(III) for 4 days at 37°C had no significant influence (P>0.05) upon ThT fluorescence relative to IAPP alone (**Figure 1**). The presence of Zn(II) significantly (P<0.05) reduced ThT fluorescence relative to IAPP alone at each metal:peptide ratio, for example, from 77(13) for IAPP only to 51(10) in the presence of only 1 μM added Zn(II) (**Figure 1**). Increasing the [Zn] up to 10 μM did not result in further statistically significant reductions in ThT fluorescence. The co-incubation of 5 μM IAPP with Cu(II) resulted in significant (P<0.05) reductions in ThT fluorescence relative to IAPP only at each metal:peptide ratio (**Figure 1**). For example, from 63(5) for IAPP only to 32(14) in the presence of only 1 μM added Cu(II). The latter was significantly (P<0.05) reduced further to 16(3) and 11(2) for [Cu] of 5 and 10 μM respectively. Reductions in ThT fluorescence in the presence of Cu(II) were significantly (P<0.05) greater than for Zn(II) for each metal:peptide ratio (**Figure 1**).

When the co-incubation of 5 μM IAPP with Al(III) was continued for 36 days at 37°C there were no significant (P>0.05) differences in ThT fluorescence between IAPP only and [Al] up to 10 μM (**Figure 2**). However, the addition of 10 μM Cu(II) to each of the treatments followed by incubation at 37°C for a further 24h resulted in statistically significant (P<0.05) reductions in ThT fluorescence for each of the metal:peptide ratios (**Figure 2**).

Influence of metal:peptide seeds on immediate aggregation of ProIAPP

All treatments were mixed by brief vortexing prior to sampling for ThT fluorescence. When ProIAPP stock was diluted

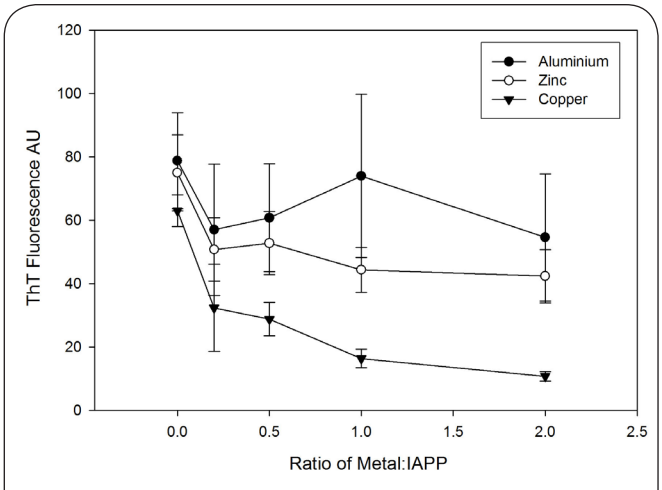

Figure 1. The influence of the concentration of Al(III), Zn(II) or Cu(II) on ThT fluorescence of a 5.0 μM IAPP preparation following 4d incubation at 37°C. Mean and SD are plotted, n=5.

doi: 10.7243/2050-0866-4-4

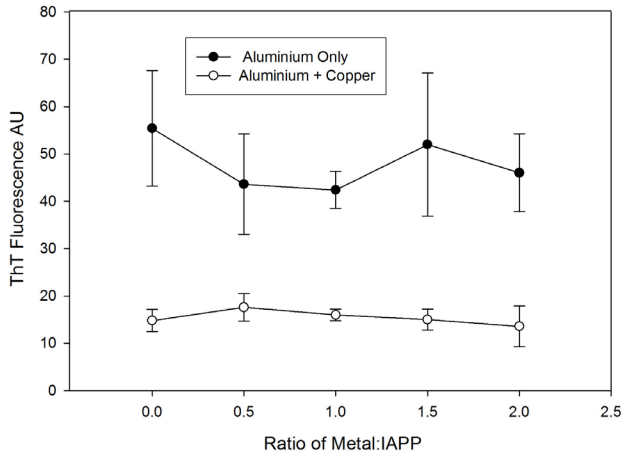

Figure 2. The upper plot shows the influence of the concentration of Al(III) on ThT fluorescence of a 5.0 μM IAPP preparation after incubation at 37°C for 36d. Mean and SD are plotted, n=5. The lower plot shows the influence on ThT fluorescence of adding Cu(II) to a concentration of 10 μM to the aged IAPP preparations and incubating them for a further 24h at 37°C. Mean and SD are plotted, n=5.

into modified KH buffer to give a final, fully mixed peptide concentration of 35 μM and allowed to equilibrate at 37°C for 600s it resulted in a steady ThT fluorescence of 19.5(11.0) for n=75 separate treatments. The addition of peptide/metal seeds to the 35 μM ProIAPP preparation resulted in statistically significant (P<0.05) increases in ThT fluorescence in every case (**Figure 3**). This included the control (5 μL of KH buffer) which following addition and mixing resulted after 600s in a stable ThT fluorescence of 74.5(32.1). A similar increase, up to 78.8(31.5), was observed for the Cu(II)/peptide seed while the peptide only, Zn(II)/peptide and Al(III)/peptide seeds resulted in statistically significant (P<0.05) higher values, 139.6(49.7), 125.6(38.0) and 155.6(38.0) respectively.

Influence of metal:peptide seeds on aggregation of ProIAPP over 49d

All treatments were mixed by brief vortexing prior to sampling for ThT fluorescence and TEM. When ProIAPP stock was diluted into modified KH buffer to give a final, fully mixed peptide concentration of 10 μM and allowed to equilibrate at 37°C for 48h it resulted in a steady ThT fluorescence of 8.8(1.8) for n=25 separate treatments. Further incubation for 7d following the addition of metal:peptide seeds (or a sham seed volume of buffer for the no seed treatment) produced significant (P<0.05) increases in ThT fluorescence for all treatments except the Cu(II)/peptide seed (**Figure 4**). For example, seeding with Al(III)/peptide resulted in ThT fluorescence of 28.7(3.1) while seeding with Cu(II)/peptide resulted in ThT fluorescence of 12.4(2.9) for n=5 replicates in each case. While the Zn(II), Al(III) and ProIAPP seeded treatments were all statistically higher (P<0.05) than either the Cu(II) or no seed treatments, they were not statistically different (P>0.05) from each other. After incubation for 14d there were no statistically significant (P>0.05) changes in ThT fluorescence for all treatments while after 49d the highest values of ThT fluorescence were observed in, the no seed treatment, 43.5(6.4), the Al(III)/peptide seed, 41.1(6.0) and the peptide only seed, 37.4(4.6). The Cu(II) and Zn(II)/peptide seeds gave similar fluorescence values which were statistically lower (P<0.05) than those for the no seed and the Al(III)/peptide seed (**Figure 4**).

TEM of the unseeded treatment at 49d showed abundant

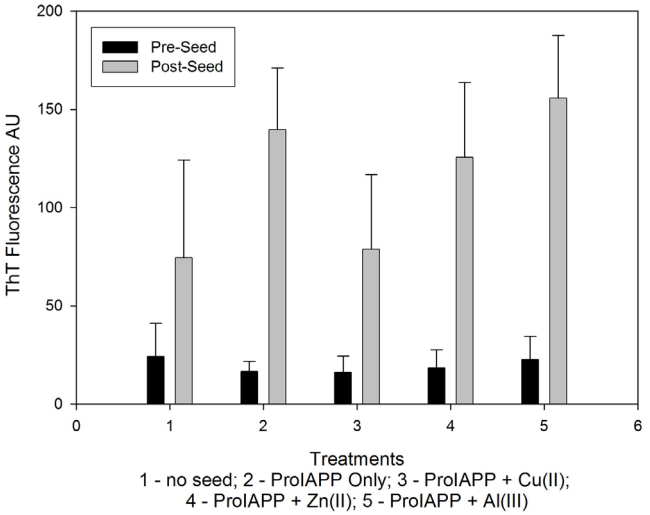

Figure 3. The influence of seeding (seeds labelled 1-5) on ThT fluorescence of a 35 μM preparation of $ProIAPP_{1-48}$ following incubation at 37°C for 600s. Mean and SD are plotted, n=15.

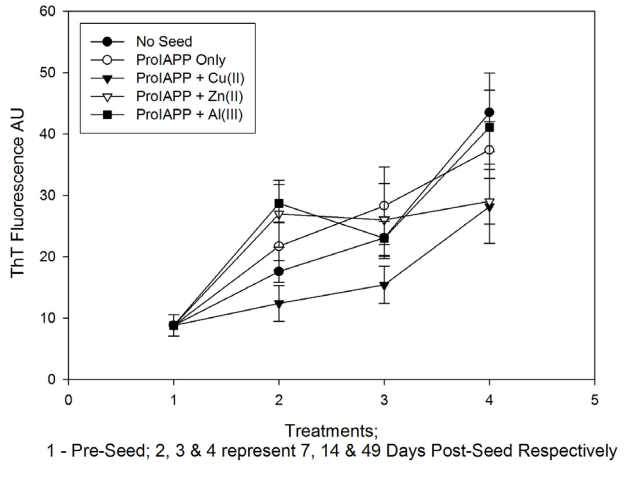

Figure 4. The influence of seeding on ThT fluorescence of a 10 μM preparation of $ProIAPP_{1-48}$ which had been incubated for 48h at 37°C (T1) and following further incubation at 37°C for 7, 14 and 49d post addition of seed (T2-4). Mean and SD are plotted, n=25 for T1 and n=5 for T2-4.

doi: 10.7243/2050-0866-4-4

negatively-stained fibrils with a mean diameter of 8.9(1.8) nm, n=25 (**Figure 5A**). TEM of the Zn(II)/peptide seeded treatment showed distinctive negatively-stained single (mean diameter 10.8(3.0) nm, n=25) and double fibrils (mean diameter 15.3(3.6) nm, n=25) (**Figure 5B**). TEM of the Cu(II)/peptide seeded treatment also showed negatively-stained single (mean diameter 7.1(1.9) nm, n=25) and double fibrils (mean diameter 13.2(3.4) nm, n=25) as well as deposits of more amorphous positively-stained peptide deposits (**Figure 5C**). TEM of the Al(III)/peptide seeded treatment showed only a few negatively-stained single fibrils (mean diameter 8.8(2.5) nm, n=25) and diffuse deposits of positively stained peptide deposits (**Figure 5D**). TEM of the peptide only seeded treatment showed a range of primarily negatively-stained fibrils. They were short, perhaps truncated, single fibrils (mean diameter 8.7(3.1) nm, n=25) (**Figure 5E**) as well as longer single (mean diameter 8.5(2.8) nm, n=25) and double fibrils (mean diameter 19.5(3.3) nm, n=25) (**Figure 5F**).

The influence of metals on IAPP aggregation over 60 minutes

Aggregation phenomena when *ca* 200 μM IAPP stock was diluted without any prior mixing to a final assay concentration of 5 μM into physiologically-significant milieu which included metals were followed over 60min by dynamic light scattering (DLS), transmission electron microscopy (TEM) and ThT fluorescence (first 15min. only). Note there was no prior mixing by vortexing or any other means for any of these preparations.

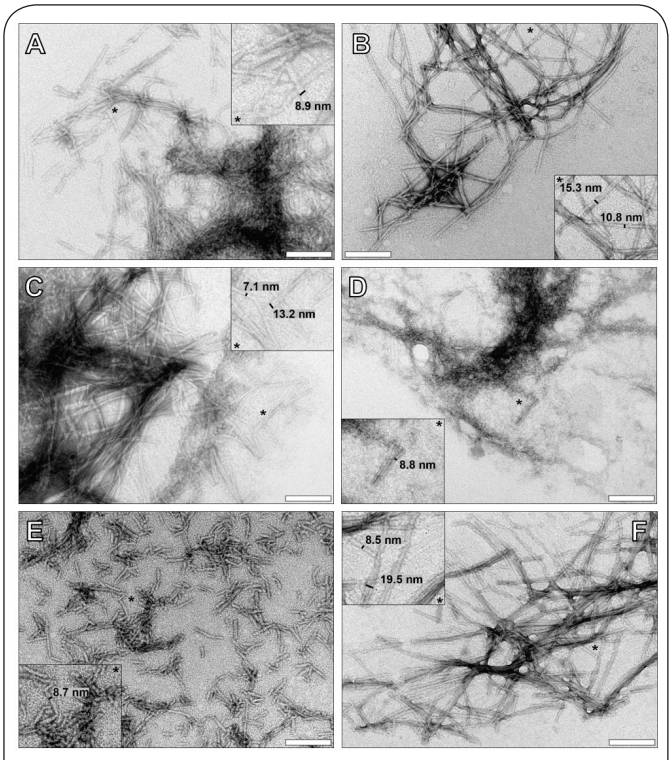

Figure 5A-F. Electron micrographs of 10μM ProIAPP$_{1-48}$ prepared in physiological Krebs Henseleit (KH) medium at pH 7.40±0.05 following 49 days incubation at 37°C. Treatments were seeded in the absence (**A**) and presence of ProIAPP$_{1-48}$ includingZn(II) (**B**), Cu(II) (**C**), Al(III) (**D**), or no added metal (**E** & **F**). Asterisk indicates the position of the magnified insert in which dimensions for single and double fibrils are shown in nm. Magnification X 100 K, all scale bars 200 nm.

IAPP in the absence of added metal produced 3 distinct particle sizes (peaks) at *ca* 1.4, 1.6 and 2.3 μm during the first 15min. period. There were no peaks representing peptide particles in the sub-micron range (**Supplement Figure S1a**). ThT fluorescence during this period showed a steady rise from *ca* 50 AU at T=0 to *ca* 80 AU at T=15min (**Supplement Figure S2a**). TEM revealed no clear fibril-like structures during this time period. Over the next 15min. peaks were observed at ca 1, 78, 570 and 900 nm and 1.2, 4.2 and 5.2 μm. Between 30 and 45min. there were particles at 327 nm and 3.6, 4.0, 5.2 and 5.7 μm. For the final 15 minutes there was evidence of disaggregation, significant peaks were observed at *ca* 500, 550, 780 and 900 nm and 2.6, 3.3 and 4.2 μm. TEM revealed fibril-like materials (width 7.74±1.42 nm) at T=30 and 60min. which were not negatively stained (**Figure 6A**).

When these experiments were repeated in the presence of 1 mM added citrate and compared to data in the absence of citrate there were overall reductions in particle sizes and specifically for the period 15-45min., statistically significant ($P<0.05$) increases in ThT fluorescence, *ca* 150 AU at T=0 to 200 AU at T=15min. (**Supplement Figure S2a**), and TEM revealed fibril-like structures (width 9.57±1.74 nm) at T=0 and T=30 (**Figure 6B**) with the latter demonstrating negative staining. At T=60min. no fibril-like materials were observed.

IAPP in the presence of equimolar added Al(III) produced no distinct particles during the initial 15min. period (**Supplement Figure S1a**). ThT fluorescence during this period showed a steady rise from *ca* 50 AU at T=0 to *ca* 110 AU at T=15min. (**Supplement Figure S2b**). TEM for this period revealed fibril-like structures which were not negatively stained. Over the next 15min. discrete particles of diameters 188, 327, 718 and 864 nm were observed. After 45min. only two discrete particles were observed of 129 and 248 nm and during the final 15min. the only particles identified were 197 nm and 4.4 μm in diameter (**Supplement Figure S1a)**. Negatively-stained fibrils were observed by TEM at T=30min. (width 4.37±0.41 nm) (**Figure 6D**) while at T=60min. no fibril-like materials were observed.

When these experiments were repeated in the presence of 1 mM added citrate and compared to data in the absence of citrate there were no clear differences in particle size distributions, no significant differences in ThT fluorescence for T=0-15min. (**Supplement Figure S2b**) while TEM showed fibril-like structures which were not negatively-stained at T=0 and 30min. (width 8.98±1.82 nm) (**Figure 6G**).

IAPP in the presence of equimolar added Cu(II) produced, after 15 min., a single peak attributed to a particle size of *ca* 1.0 μm in diameter (**Supplement Figure S1b**). ThT fluorescence during the same period showed a steady increase from 30 AU at T=0 to 50 AU at T=15min. (**Supplement Figure S2c**) while

doi: 10.7243/2050-0866-4-4

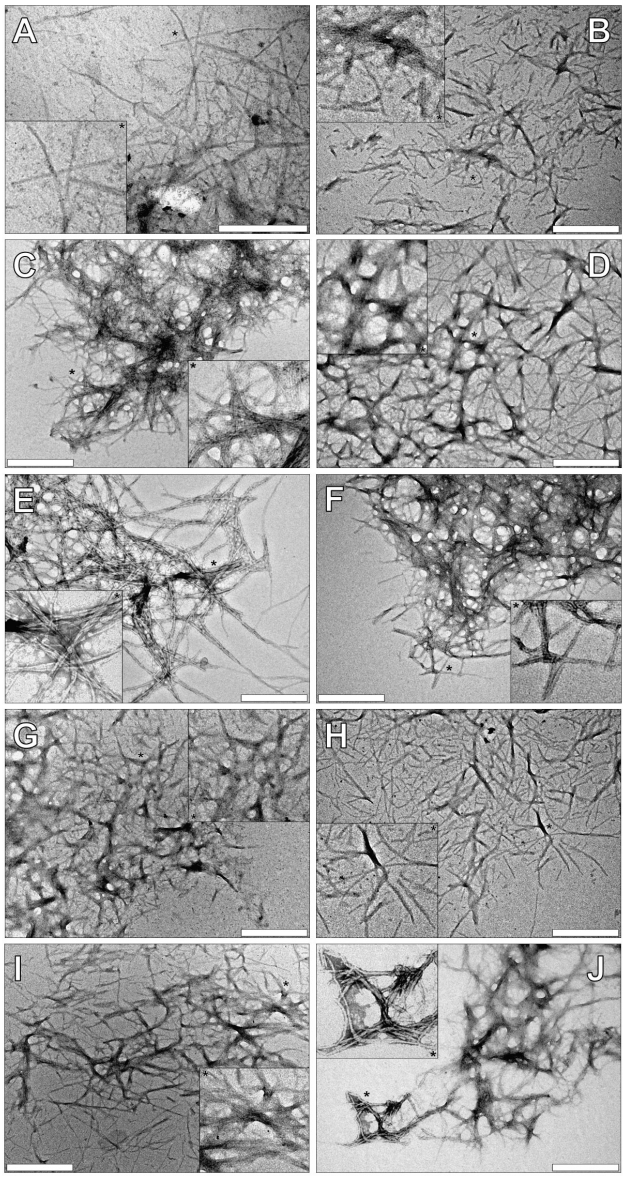

Figure 6A-J. Electron micrographs of 5μM IAPP1-37 prepared in physiological Krebs Henseleit (KH) medium at pH 7.40±0.05 following 0, 30 or 60min. at 37°C. Treatments were prepared in the absence (**A** & **B**) or presence of 5μM Al(III) (**C** & **D**), Fe(III) (**E** & **F**), Cu(II) (**G** & **H**) or Zn(II) (**I** & **J**), containing KH medium only (**A**, **C**, **E**, **G** & **I**) or KH medium including 1mM citrate (**B**, **D**, **F**, **H** & **J**). Amyloid fibril formation is shown at 30min. for all treatments, except where negative staining was observed at T=0 (J) or 60min. (**F**). Asterisk indicates the position of the magnified insert. Magnification X 80 K (**A**), X 60 K (**B**–**J**). All scale bars 500 nm.

TEM revealed fibril-like material which was not negatively-stained. After 30min. a sub-nanometre particle of ca 0.6 nm was observed as well as particles of 1, 550, 650 and 990 nm. TEM at 30min. revealed non-negatively-stained fibril-like structures (width 8.81±1.03 nm) similar to those also seen at T=0 (**Figure 6G**). Over the next period, 30-60min. a wide range of particles were observed of diameters 0.3, 0.7, 0.8, 1, 2, 16, 130, 164, 350, 625, 825, 948 nm and 1.2 and 4.2 μm (**Supplement Figure S1b**). At T=60min. no fibril-like structures were observed by TEM.

When these experiments were repeated in the presence of 1 mM added citrate and compared to data in the absence of citrate there were many larger particles observed at earlier time points to the extent that between 45-60min. no particles <6 μm in diameter were observed. Citrate increased ThT fluorescence significantly (P<0.05) to *ca* 150 AU at T=15min. (**Supplement Figure S2c**) while having no clear influence on the non-negatively-stained fibril-like structures (width 9.13±1.35 nm) observed by TEM at T=0 and 30min. (**Figure 6H**). At T=60min. no fibril-like structures were observed by TEM.

IAPP in the presence of equimolar added Zn(II) immediately produced a wide range of particle sizes including diameters of 0.5, 1, 544, 686 and 948 nm and 1.3 and 1.7 μm (**Supplement Figure S1c**). ThT fluorescence during this initial 15min. period increased slowly from *ca* 30 AU to 80AU (**Supplement Figure S2d**) while non-negatively-stained fibril-like structures were observed by TEM. A similarly wide range of particle diameters were also evident after 30min. including, 0.4, 0.9, 1, 570, 600, 690, 825 and 990 nm and 1.1, 1.3, 1.7, 2.6 and 3.6 μm. Between 30-45min. particles of diameters 0.2, 0.3, 0.8, 136, 149, 718 and 992 nm and 4.0 μm were observed. During the final 15min. period particles were observed of diameters 0.7, 0.8, 1.0, 260 and 452nm and 2.2, 2.9, 4.6 and 4.8 μm (**Supplement Figure S1c**). Non-negatively-stained fibril-like structures (width 9.05±1.87 nm) were observed at T=30 and T=60min. by TEM (**Figure 6I**).

When these experiments were repeated in the presence of 1 mM added citrate and compared to data in the absence of citrate the particle size distribution data indicated either overall reductions in the size of particles or their aggregation towards particle diameters >6.0 μm. The non-significant (P>0.05) increase in ThT fluorescence at T=15min. from *ca* 80 AU to 140 AU (**Supplement Figure S2d**) might favour the latter while TEM showing negatively-stained fibrils at T=0 (**Figure 6J**) and T=30min. and non-negatively stained fibril-like structures at T=60min. would also support this.

IAPP in the presence of equimolar added Fe(III) at T=15min. resulted in just one single discrete particle of 825 nm diameter (**Supplement Figure S1d**). ThT fluorescence increased during this period from *ca* 50 AU up to a maximum of 350 AU at T=15min. for one replicate (**Supplement Figure S2e**). TEM at T=0 revealed negatively stained fibrils (width 6.21±0.78 nm). Between 15-45min. particles of diameter 0.8, 1.1, 1.4, 1.7, 2.2 and 3.2 μm were observed while the range of particle sizes increased significantly during the final 15min. period to include particles of sub-nanometre, 0.02 and 0.75 nm, nanometre, *ca* 1.0, 2.0, 35.0, 40.0, 94.0, 379.0, 625.0 and 686.0 nm and micrometre, 1.0, 3.8 μm diameters. At T=30min. there were

doi: 10.7243/2050-0866-4-4

clear negatively-stained fibrils while at T=60min. no fibril-like deposits were observed by TEM (**Figure 6E**).

When these experiments were repeated in the presence of 1 mM added citrate and compared to data in the absence of citrate the particle sizes were reduced across the full 60min. time period. ThT fluorescence was unaffected by the presence of citrate while TEM showed no deposits at T=0, dense non-negatively-stained fibril-like structures at T=30min. and similarly dense but negatively-stained fibrils (width 10.61±1.72 nm) at T=60min. (**Figure 6F**).

Discussion

Metals and IAPP

The dilution of a 200 μM stock of IAPP into a physiologically-relevant medium to a final peptide concentration of 5 μM following mixing by vortexing and incubation for 4d at 37°C resulted in ThT fluorescence of 60-80 AU and indicated the formation of β sheets of this amyloidogenic peptide. The additional presence of up to 10 μM Al(III) had no significant influence upon ThT fluorescence even when the period of incubation was extended to 36d. Both Zn(II) and Cu(II) reduced ThT fluorescence of 5 μM IAPP only treatments and significantly so from only 1 μM added metal. Both metals at sub-stoichiometric concentrations prevented IAPP from forming β sheets while Cu(II) also abolished the ThT fluorescence of β sheets of IAPP pre-formed in the absence and presence of added Al(III).

Previous research on IAPP showed that in the presence of stoichiometric excesses of metal, Al(III) and Zn(II) increased, Cu(II) decreased and Fe(III) had no influence upon ThT fluorescence under near-physiological conditions [**3**]. The influence of Cu(II) in preventing IAPP from forming β sheet structures has since been confirmed [**5-8**]. However, subsequent research for Zn(II), under experimental conditions further from physiological, showed that significant excesses of Zn(II) reduced ThT fluorescence of IAPP [**5**]. Herein we report the first data for stoichiometric and sub-stoichiometric concentrations of metals and while we confirmed the inhibitive action of Cu(II), and to a lesser extent Zn(II) we did not see any influence of Al(III).

Seeded aggregation of ProIAPP

ProIAPP$_{1\text{-}48}$ at a concentration of 35 μM is mildly amyloidogenic forming ThT-reactive amyloid, *ca* 20 AU, after incubation under near-physiological conditions for 600s. Seeding of this preparation of ProIAPP$_{1\text{-}48}$ with 'seeds' prepared from ProIAPP$_{1\text{-}48}$ or ProIAPP$_{1\text{-}48}$ in the presence of equimolar Al(III), Zn(II) or Cu(II) produced statistically significant increases in ThT fluorescence over a further 600s incubation period and especially for seeds prepared from peptide only and peptide plus Al(III) or Zn(II). However, a 'sham' seed composed of only physiological buffer also resulted in a statistically significant increase in ThT fluorescence, the same as the peptide-Cu(II) seed but significantly lower than solutions seeded with ProIAPP$_{1\text{-}48}$ only or peptide plus Al(III) or Zn(II). The result of the sham seeding suggested that simple disruption and mixing of the ProIAPP$_{1\text{-}48}$ was sufficient to induce further aggregation of the peptide over the short term and that the increase in ThT fluorescence observed for the peptide-Cu(II) seed was a mixing phenomenon.

The seeding effects seen for ProIAPP$_{1\text{-}48}$ and peptide plus Al(III) or Zn(II) were also observed for similar preparations which had been aged for 7d. However, incubation for 14d and thereafter 49d negated all seeding effects and the highest ThT fluorescence was observed in the unseeded peptide preparation. Negatively stained fibrils were observed by TEM in all treatments after incubation for 49d. There were clear differences in fibril morphologies between the different seeded treatments which though suggesting that seeding was influential the influences were not seemingly related to ThT fluorescence. In summary these results have suggested that while seeding amyloid preparations can catalyse the formation of ThT-reactive amyloid in the short term some of the catalysis can be attributed to simple mixing phenomena and, importantly, the catalytic effects are relatively short-lived, at least with respect to formation of ThT-reactive amyloid.

Seeding of amyloid aggregation has been implicated in a number of amyloid-related pathologies [**12**,**13**]. However, there are very few studies in relation to self-seeding of IAPP [**14**] and no previous research on ProIAPP$_{1\text{-}48}$. A previous study on IAPP suggested that seeding abolished a lag phase in amyloid formation without influencing total amyloid formation [**14**] and we observed something similar for ProIAPP$_{1\text{-}48}$ herein. However, 'lag' phases in amyloid formation are rarely observed under-near physiological conditions [**4**,**15**] and what we observed were increases in the rate of formation of β sheets of amyloid which also occurred, if to a lesser extent, following sham seeding. The latter are rarely used controls in previous studies on amyloid seeding. While different seeding environments resulted in different fibril morphologies after incubation for 49d at 37°C they did not result in different ThT-reactive fluorescence, with the exception of the Cu(II)-ProIAPP$_{1\text{-}48}$ seed which resulted in significantly lower ThT fluorescence as might be expected from the additional presence of Cu(II) in the assay [**4**]. These data tend to cast some doubt over a significant role for self-seeding in the formation of β sheets of ProIAPP$_{1\text{-}48}$ in relation to their putative cytotoxicity in type 2 diabetes mellitus.

Aggregation of IAPP

Since machine mixing of amyloid preparations prior to investigating their aggregation phenomena may be somewhat artificial in relation to what happens *in vivo* when concentrated peptide preparations are released into various extracellular milieus the aggregation of IAPP was investigated without any prior mixing. It was intriguing for IAPP only (Al(III), Cu(II), Zn(II) or Fe(III) not added to physiological media) that during the first 15min. (during which one assumed that the peptide stock diluted into the physiological medium) only micron-

doi: 10.7243/2050-0866-4-4

sized particles were observed by DLS and while they were accompanied by a strong ThT fluorescence there were no fibril-like materials observed by TEM for this period. Over the next 30min. a wide range of particle sizes were identified by DLS and included both sub-micron and micron-sized peaks which together seemed to indicate *de novo* aggregation phenomena though the fibril-like materials identified by TEM were not negatively stained. This was also true of fibril-like materials identified at T=60min. and DLS data suggested some disaggregation of amyloid aggregates during the final period of the 60 min. assay. When these experiments were repeated in media which additionally included 1 mM citrate there were some clear differences including overall reductions in the size of amyloid aggregates which were accompanied by statistically significant ($P<0.05$) increases in ThT fluorescence and the distinct presence of negatively-stained fibrils. These fibrils were significantly wider (9.57 against 7.74 nm) than in the absence of citrate. The changes caused by citrate must be attributable to the binding of low concentrations of contaminating metals, these metals seemingly promoting the rapid aggregation of non-negatively stained amyloid.

The presence of equimolar Al(III) appeared to both slow down aggregation of the peptide and limit the range of particle sizes. There were small increases in ThT fluorescence and these were accompanied by early observations of negatively-stained fibrils of mean diameter of only 4.37nm. The additional presence of citrate while having no clear influence upon particle sizes or ThT fluorescence did result in fibrillar materials which were not negatively-stained and were significantly wider at *ca* 9nm. Equimolar Cu(II) produced the expected reductions in ThT fluorescence which were accompanied by evidence of slow aggregation kinetics involving a wide range of particle sizes. The fibril-like materials viewed by TEM were not negatively stained and the additional presence of citrate while not affecting fibril morphology did appear to significantly increase the rate of aggregation of all structures such that there were none visible to DLS (<6 μm) or TEM at T=60 minutes. These changes were accompanied by significant increases in ThT fluorescence presumably indicating binding of Cu(II) by citrate. The presence of equimolar Zn(II) resulted in both nanoscale and micron-sized particles of IAPP almost from T=0 with these particles being identified throughout the 60min. assay. The aggregation phenomena were accompanied by low but slowly increasing ThT fluorescence as well as non-negatively-stained fibrillar materials at T=30 and 60 minutes. The additional presence of citrate, which might be expected to bind Zn(II), resulted in non-significant increases in ThT fluorescence and of most interest the presence of negatively-stained fibrils at both T=0 and T=30 minutes. Equimolar Fe(III) resulted in almost exclusively micron-sized particles for the first 45min. and observations by TEM revealed negatively-stained fibrils at both 0 and 30minutes. The early presence of negatively-stained fibrils was further supported by an increase in ThT fluorescence during the first 15min. period. During the final 15min. period of the assay a range of sub-micron particles were observed by DLS which suggested either *de novo* aggregation of monomeric peptide or potentially dissolution of micron-sized peptide aggregates. Interestingly the additional presence of citrate reduced the average particle size over the whole assay period without influencing ThT fluorescence though under these conditions negatively-stained fibrils, and hence assumed to be β-pleated sheet structures, were only visible by TEM at 60min. and not at either of the earlier time points.

We are not aware of any other research in which the aggregation of IAPP was followed by 3 different techniques for the first 60min. after an IAPP stock was diluted into a near-physiological milieu without additional mixing. It is probably true to say that such data do not exist for any amyloid-forming peptide and especially for media including physiologically-relevant concentrations of metals. There are data which suggest that a sub-stoichiometric concentration of Cu(II) incubated with IAPP for 48h at room temperature reduced the size of IAPP particles from predominantly micron-sized to predominantly sub-micron [9] and the slower aggregation kinetics observed in our equimolar Cu(II)-IAPP preparations could support such an influence of Cu(II) on IAPP particle sizes. Overall the data suggest that equimolar Al(III), Fe(III) and Zn(II) all accelerated the aggregation of $ProIAPP_{1-48}$ towards micron-sized particles or clusters while Cu(II) may have had the opposite effect. These qualitative observations will require confirmation in future research and significantly in preparations where metals are also present to excess. Perhaps more significant physiologically was that metals changed the morphologies of the resultant fibrillar materials producing both a range of fibril diameters, with Al(III) having the most dramatic effect, and negatively-stained and non-negatively stained structures.

Additional files

Supplementary figure S1
Supplementary figure S2

Competing interests

The authors declare that they have no competing interests.

Authors' contributions

Authors' contributions	MM	CB	PG	AR	CR	NT	HT	LW	PEF	CE
Research concept and design	--	--	--	--	--	--	--	--	✓	✓
Collection and/or assembly of data	✓	✓	✓	✓	✓	✓	✓	✓	--	--
Data analysis and interpretation	✓	✓	✓	✓	✓	✓	✓	--	--	✓
Writing the article	--	✓	--	--	--	--	--	--	✓	✓
Critical revision of the article	✓	--	--	--	--	--	--	--	✓	✓
Final approval of article	✓	✓	✓	✓	✓	✓	✓	✓	✓	✓

Acknowledgement
PEF acknowledges support from the Canadian Institute for Health Research.

Publication history
Senior Editor: Lu Cai, University of Louisville, USA.
EIC: Geoffrey Burnstock, University College London, UK.
Received: 11-Nov-2015 Final Revised: 05-Dec-2015
Accepted: 11-Dec-2015 Published: 23-Dec-2015

Citation:
Mold M, Bunrat C, Goswami P, Roberts A, Roberts C, Taylor N, Taylor H, Wu L, Fraser PE and Exley C. **Further insight into the role of metals in amyloid formation by $IAPP_{1-37}$ and $ProIAPP_{1-48}$**. *J Diab Res Clin Met*. 2015; **4**:4.
http://dx.doi.org/10.7243/2050-0866-4-4

References

1. Knowles TP, Vendruscolo M and Dobson CM. **The amyloid state and its association with protein misfolding diseases**. *Nat Rev Mol Cell Biol*. 2014; **15**:384-96. | Article | PubMed
2. Fernandez MS. **Human IAPP amyloidogenic properties and pancreatic beta-cell death**. *Cell Calcium*. 2014; **56**:416-27. | Article | PubMed
3. Ward B, Walker K and Exley C. **Copper(II) inhibits the formation of amylin amyloid in vitro**. *J Inorg Biochem*. 2008; **102**:371-5. | Article | PubMed
4. Exley C, Mold M, Shardlow E, Shuker B and Ikpe B et al. **Copper in a potent inhibitor of the propensity for human $ProIAPP_{1-48}$ to form amyloid fibrils in vitro**. *J Diab Res ClinMetab*. 2012, **1**:3. | Article
5. Brender JR, Hartman K, Nanga RP, Popovych N, de la Salud Bea R, Vivekanandan S, Marsh EN and Ramamoorthy A. **Role of zinc in human islet amyloid polypeptide aggregation**. *J Am Chem Soc*. 2010; **132**:8973-83. | Article | PubMed Abstract | PubMed Full Text
6. Sinopoli A, Magri A, Milardi D, Pappalardo M, Pucci P, Flagiello A, Titman JJ, Nicoletti VG, Caruso G, Pappalardo G and Grasso G. **The role of copper(II) in the aggregation of human amylin**. *Metallomics*. 2014; **6**:1841-52. | Article | PubMed
7. Li H, Ha E, Donaldson RP, Jeremic AM and Vertes A. **Rapid Assessment of Human Amylin Aggregation and Its Inhibition by Copper(II) Ions by Laser Ablation Electrospray Ionization Mass Spectrometry with Ion Mobility Separation**. *Anal Chem*. 2015; **87**:9829-37. | Article | PubMed Abstract | PubMed Full Text
8. Riba I, Barran PE, Cooper GJS and Unwin RD. **On the structure of the copper-amylin complex**. *Int J Mass Spec*. 2015. | Article
9. Ma L, Li X, Wang Y, Zheng W and Chen T. **Cu(II) inhibits hIAPP fibrillation and promotes hIAPP-induced beta cell apoptosis through induction of ROS-mediated mitochondrial dysfunction**. *J Inorg Biochem*. 2014; **140**:143-52. | Article | PubMed
10. House E, Collingwood J, Khan A, Korchazkina O, Berthon G and Exley C. **Aluminium, iron, zinc and copper influence the in vitro formation of amyloid fibrils of Abeta42 in a manner which may have consequences for metal chelation therapy in Alzheimer's disease**. *J Alzheimers Dis*. 2004; **6**:291-301. | Article | PubMed
11. House E, Mold M, Collingwood J, Baldwin A, Goodwin S and Exley C. **Copper abolishes the beta-sheet secondary structure of preformed amyloid fibrils of amyloid-beta(42)**. *J Alzheimers Dis*. 2009; **18**:811-7. | Article | PubMed Abstract | PubMed Full Text
12. Jarrett JT and Lansbury PT, Jr. **Seeding "one-dimensional crystallization" of amyloid: a pathogenic mechanism in Alzheimer's disease and scrapie?** *Cell*. 1993; **73**:1055-8. | Article | PubMed
13. Walker LC and Jucker M. **Neurodegenerative diseases: expanding the prion concept**. *Annu Rev Neurosci*. 2015; **38**:87-103. | Article | PubMed
14. Tu LH and Raleigh DP. **Role of aromatic interactions in amyloid formation by islet amyloid polypeptide**. *Biochemistry*. 2013; **52**:333-42. | Article | PubMed Abstract | PubMed Full Text
15. Mold M, Ouro-Gnao L, Wieckowski BM and Exley C. **Copper prevents amyloid-beta(1-42) from forming amyloid fibrils under near-physiological conditions in vitro**. *Sci Rep*. 2013; **3**:1256. | Article | PubMed Abstract | PubMed Full Text